Journal of Environmental Radioactivity 124 (2013) 205–213

Contents lists available at SciVerse ScienceDirect

Journal of Environmental Radioactivity

journal homepage: www.elsevier.com/locate/jenvrad

Monitoring rainwater and seaweed reveals the presence of ^{131}I in southwest and central British Columbia, Canada following the Fukushima nuclear accident in Japan

A. Chester [a,*], K. Starosta [a,**], C. Andreoiu [a], R. Ashley [a], A. Barton [b], J.-C. Brodovitch [a], M. Brown [a], T. Domingo [a], C. Janusson [c], H. Kucera [c], K. Myrtle [d], D. Riddell [c], K. Scheel [b], A. Salomon [e], P. Voss [a]

[a] Simon Fraser University, Department of Chemistry, 8888 University Drive, Burnaby, BC, Canada V5A 1S6
[b] Simon Fraser University Radiation Safety, 8888 University Drive, Burnaby, BC, Canada V5A 1S6
[c] Bamfield Marine Sciences Centre, 100 Pachena Road, Bamfield, BC, Canada V0R 1B0
[d] Simon Fraser University Department of Physics, 8888 University Drive, Burnaby, BC, Canada V5A 1S6
[e] Simon Fraser University School of Resource and Environmental Management, 8888 University Drive, Burnaby, BC, Canada V5A 1S6

ARTICLE INFO

Article history:
Received 20 February 2013
Received in revised form
7 May 2013
Accepted 31 May 2013
Available online

Keywords:
Fukushima
Radiation monitoring
Seaweed
Detector development

ABSTRACT

Detailed analysis of ^{131}I levels in rainwater and in three species of seaweed (*Fucus distichus* Linnaeus, *Macrocystis pyrifera*, and *Pyropia fallax*) collected in southwest British Columbia and Bella Bella, B.C., Canada was performed using gamma-ray spectroscopy following the Fukushima nuclear power plant accident on March 11, 2011. Maximum ^{131}I activity was found to be 5.8(7) Bq/L in rainwater collected at the campus of Simon Fraser University in Burnaby, B.C. nine days after the accident. Concomitantly, maximum observed activity in the brown seaweed *F. distichus* Linnaeus was observed to be 130(7) Bq/kg dry weight in samples collected in North Vancouver 11 days following the accident and 67(6) Bq/kg dry weight in samples collected from the Bamfield Marine Sciences Centre on Vancouver Island 17 days following the accident. The ^{131}I activity in seaweed samples collected in southwest B.C. following the Fukushima accident was an order of magnitude less than what was observed following Chernobyl. Iodine-131 activity in *F. distichus* Linnaeus remained detectable for 60 days following the accident and was detectable in each seaweed species collected. The Germanium Detector for Elemental Analysis and Radioactivity Studies (GEARS) was modeled using the GEANT4 software package and developed as an analytical tool by the Nuclear Science group in the Simon Fraser University Department of Chemistry for the purpose of these measurements.

1. Introduction

Following the Tōhoku earthquake and subsequent tsunami on March 11, 2011, the damaged Fukushima Dai-ichi nuclear power plant released radioisotopes from fission fragments and nuclear fuel into the environment. Some fission fragments were released as aerosols or gasses and dispersed over a large geographic region through the atmosphere. The volatile fission fragment ^{131}I represents ~2.89% of the fission yield of enriched uranium (England and Rider, 1994) and is of particular concern to human health due to accumulation in the thyroid. Iodine-131 is not naturally present in the environment, but with an 8.0252 day half-life (National Nuclear Data Center Interactive Chart of Nuclides, 2012), survives long enough to be transported in the atmosphere across the Pacific Ocean. Therefore, during the current studies any ^{131}I detected in rainwater or seaweed was attributed to releases from Fukushima.

Fallout of ^{131}I following the Fukushima accident was widespread. Airborne ^{131}I was observed in Europe (Ioannidou et al., 2012; Manolopoulou et al., 2011; Perrot et al., 2012; Pham et al., 2012), the Canary Islands off the northwest coast of Africa (López-Pérez et al., 2013), South Korea (Kim et al., 2012) and in the northwest United States (Diaz Leon et al., 2011). Iodine-131 concentrations in rainwater of $\leq$ 3.5 Bq/L were reported in Bordeaux, France (Perrot et al., 2012), Milano, Italy (Ioannidou et al., 2012), and Jeju, South Korea (Kim et al., 2012). Measurements of ^{131}I in

* Corresponding author. Tel.: +1 5172309019.
** Corresponding author.
E-mail addresses: ascheste@sfu.ca (A. Chester), starosta@sfu.ca (K. Starosta).

0265-931X/$ – see front matter © 2013 Elsevier Ltd. All rights reserved.
http://dx.doi.org/10.1016/j.jenvrad.2013.05.013

Washington state, U.S.A., indicated that releases from Fukushima first arrived between March 16 and March 18. Subsequently, ^{131}I was first detected on the European continent between March 21 and March 28 and in South Korea on March 28.

As part of the global effort to monitor fission fragment releases following the Fukushima accident, ^{131}I was measured in rainwater collected at the Simon Fraser University (SFU) campus on Burnaby Mountain and in seaweed samples collected in North Vancouver, B.C., the Bamfield Marine Sciences Centre (BMSC) on Vancouver Island, B.C., located ~250 km west of Vancouver, and Bella Bella, B.C., located ~650 km north of Vancouver along the Pacific coast. The perennial brown seaweed species *Fucus distichus* Linnaeus (henceforth *Fucus*) was chosen as the primary biological monitor for ^{131}I releases from Fukushima. *Fucus* was chosen because it is known to concentrate iodine present in the environment, is widespread in intertidal zones in the Pacific Northwest where it can accumulate iodine from rainfall, and was used as a biological monitor in B.C. following the Chernobyl disaster (Druehl et al., 1988). In addition, *Macrocystis pyrifera* and *Pyropia fallax* samples collected in Bella Bella served as secondary biological monitoring systems. The monitoring campaign provided an opportunity to develop the equipment and techniques necessary to perform highly accurate analytical radiochemistry at SFU in order to assess ^{131}I contamination in B.C. following Fukushima and to compare with measurements made following the Chernobyl accident.

Iodine-131 content in rainwater and seaweed was monitored following the analysis of gamma-ray decay spectra acquired using a shielded high purity germanium (HPGe) detector. HPGe detectors possess excellent energy resolution which facilitates the detection of weak sources of radiation that would otherwise be lost in the background if detectors with poorer energy resolution, such as inorganic scintillators are used (Knoll, 2000). HPGe detectors are therefore the preferred tool to measure complex spectra such as those found in environmental samples which contain many gamma-ray lines that must be resolved for proper analysis.

2. Materials and methods

2.1. The Germanium Detector for Elemental Analysis and radiation studies

The Germanium Detector for Elemental Analysis and Radioactivity Studies (GEARS) is an Ortec GEM Profile Series HPGe coaxial gamma-ray detector which was operational at the time of the Fukushima accident. GEARS is coupled to an ORTEC DSpec jr. 2.0 multichannel analyzer (MCA) with bias voltage provided by a built-in power supply. Gamma-ray decay spectra are collected by a computer running the Ortec Maestro32 software.

Fig. 1. The GEARS detector inside the lead shielding. The Cu/Cd graded-*Z* shield is visible around the detector can at the center. Contained within the aluminum can is a cryostat which houses the HPGe crystal.

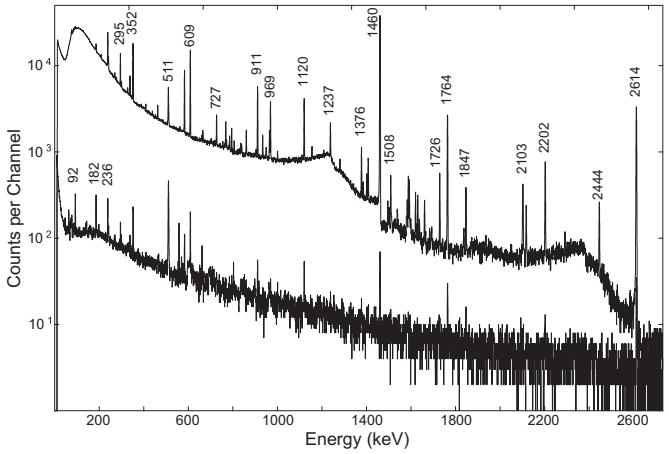

Fig. 2. Examples of background spectra obtained with GEARS in an unshielded [top] and shielded [bottom] configuration; the shielded configuration shows a ~100 fold decrease in the overall background while many background peaks associated with NORM are either eliminated or strongly suppressed. Spectra are normalized to the same livetime.

A low-activity lead shield with dimensions 51 cm × 51 cm × 64 cm ($l \times w \times h$) constructed from 10 cm thick lead bricks was used to house the GEARS detector and reduce low-level background due to naturally occurring radioactive materials (NORM) (Malain et al., 2012). The lead shield is coupled with a Cu/Cd graded-*Z* shield to decrease the flux of low energy gamma rays and X-rays from NORM and the lead shield (Knoll, 2000); this setup is shown in Fig. 1. This shielding arrangement reduces NORM background measured by the GEARS detector by a factor of ~100, see Fig. 2.

GEARS was energy calibrated with a set of standard radioactive point sources, and a function mapping the MCA channel number to energy was determined by a χ^2 fit. Absolute efficiency at 1173.237 keV and 1332.492 keV was measured using a calibrated ^{60}Co source with activity known to 1%. A linearized χ^2 fit was

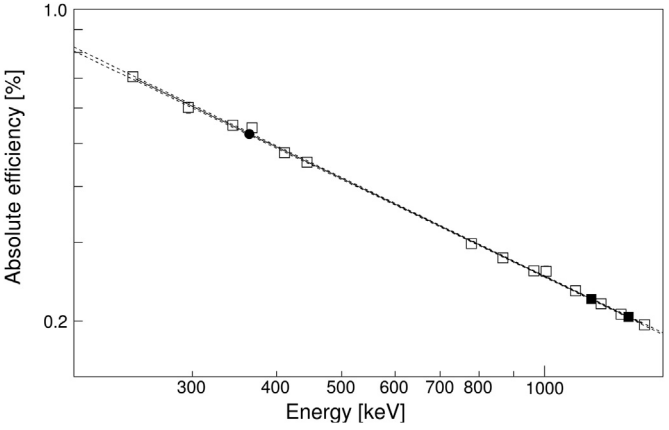

Fig. 3. Absolute efficiency of GEARS as a function of energy measured using point sources. The scaled χ^2 best fit to Eq. (1) is shown as a solid line, the 1σ confidence interval is shown as a dashed line. Data shown are ^{152}Eu [hollow squares], the absolute efficiency measured for ^{60}Co [filled squares], and calculated absolute efficiency of 0.525(6)% for the ^{131}I peak of interest [filled circle]. The data from this figure are shown in Table 1.

Table 1
Relative and absolute efficiency of GEARS for point-like radioactive sources positioned 10.5 cm above the detector can. The relative efficiency was measured from an ^{152}Eu spectrum and was scaled to the absolute efficiency measured using a calibrated ^{60}Co source; the efficiency of ^{131}I detection was calculated using Eq. (1). Errors at one standard deviation are shown in parentheses. These data are shown in Fig. 3.

Isotope	Energy [keV]	Relative efficiency [arb.]	Absolute efficiency [%]
^{152}Eu	244.692	628 (11)	0.705 (14)
^{152}Eu	295.939	536 (13)	0.602 (16)
^{152}Eu	344.276	489 (3)	0.549 (7)
^{131}I	364.489	–	0.525 (6)
^{152}Eu	367.789	483 (10)	0.542 (12)
^{152}Eu	411.115	424 (4)	0.476 (7)
^{152}Eu	443.976	404 (6)	0.454 (8)
^{152}Eu	778.903	266 (3)	0.298 (5)
^{152}Eu	867.388	247 (5)	0.277 (6)
^{152}Eu	964.131	231 (3)	0.259 (4)
^{152}Eu	1005.279	230 (5)	0.259 (7)
^{152}Eu	1112.116	208 (3)	0.234 (4)
^{60}Co	1173.237	–	0.224 (2)
^{152}Eu	1212.950	195 (2)	0.219 (4)
^{152}Eu	1299.124	184 (2)	0.207 (4)
^{60}Co	1332.492	–	0.204 (2)
^{152}Eu	1408.011	174.7 (6)	0.196 (2)

performed on a relative efficiency curve measured using a ^{152}Eu source using a power law given by Eq. (1)

$$\log \varepsilon_{\text{rel.}} = k \log E + b \tag{1}$$

where $\varepsilon_{\text{rel.}}$ is the relative efficiency, E is the energy, and k and b parametrize the line. The 1σ (68.27%) confidence interval was calculated for the best fit line and defines the error on the measured efficiency. An absolute efficiency curve in the energy range from 250 keV to 1400 keV was constructed by scaling the relative efficiency curve to the absolute efficiency measured using the calibrated ^{60}Co source; this is shown in Fig. 3. Relative and absolute efficiency values for GEARS are shown in Table 1.

An alternative, source-independent efficiency calibration method utilizing the sum peak of ^{60}Co was performed (Kim et al., 2003); a comparison between the two absolute efficiency calibration methods is shown in Table 2. There is a $\sim$5% discrepancy between the two calibration methods which is an $\sim 3\sigma$ effect. This discrepancy does not have a large impact on the presented results since it is insignificant when compared to statistical errors on the measurements. The 1% source measurement method was chosen as the calibration standard in these studies; errors in the included tables are statistical errors at one standard deviation derived from this source, though a systematic error of 5% estimated based on the sum peak method result cannot be excluded.

2.2. GEANT4 simulations

GEANT4 is a software package developed by the European Organization for Nuclear Research (CERN) to simulate the interaction of radiation with matter (Agostinelli et al., 2003; Allison et al., 2006). GEANT4 allows the user to create an experimental hall of custom dimension and incorporate objects of various geometries and materials into the hall. The GEARS detector, housing, graded-Z shield, lead shield, and other components were modeled using this framework as shown in Fig. 4. Extended radioactive sources have been implemented in GEANT4 to simulate the available sample configurations. Implemented configurations include 24 mL, 60 mL, and 120 mL glass vials.

Gamma ray self absorption in extended source samples can be simulated in GEANT4 provided that the elemental composition and density of the samples are known. Extended sources composed of water were implemented in GEANT4. The density of processed seaweed was measured from various samples; the exact elemental composition of the seaweed samples was not known and assumed to be 100% carbon for the purpose of the GEANT4 self absorption simulations. Simulations implementing gamma ray self absorption

Table 2
Comparison between absolute efficiency for the 1173.237 keV and 1332.492 keV gamma rays associated with ^{60}Co decay measured with a source activity calibrated to 1% and calculated using the sum peak method with the source secured 10.5 cm above the detector can. Efficiencies for both methods were obtained from the same experimental spectrum. Errors at one standard deviation are shown in parentheses, for further details regarding error analysis, see Sec. 2.1.

Method	$\varepsilon_{1173\text{ keV}}$	$\varepsilon_{1332\text{ keV}}$
^{60}Co source calibrated to 1%	0.224 (2)%	0.204 (2)%
Sum peak method	0.214 (2)%	0.195 (3)%

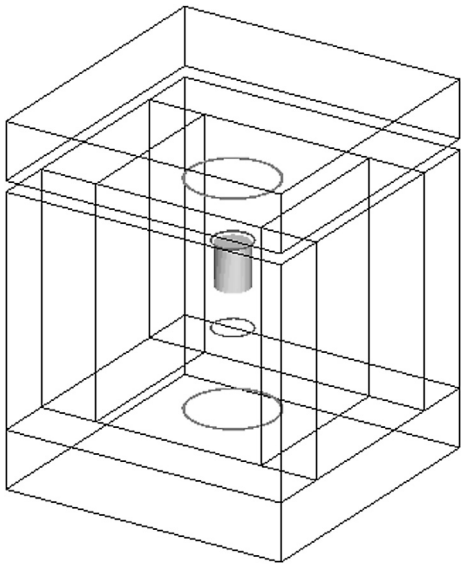

Fig. 4. The GEARS geometry implemented in the GEANT4 software package. The box superstructure is lead shielding, the large wire-frame cylinder is the Cu/Cd graded-Z shield, the small wire-frame cylinder is the aluminum can which houses the detector, and the solid cylinder is the HPGe crystal of the GEARS detector.

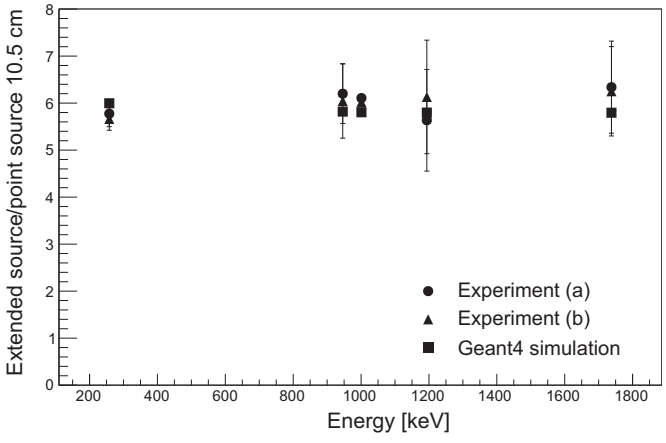

Fig. 5. Extended source/point source efficiency ratio at prominent gamma-ray energies of ^{234}U. The results from two independent experiments (a) and (b) are shown with GEANT4 simulations for the serial dilution measurements described in Sec. 2.3. Results shown are for the 24 mL vial, the initial step of the serial dilution process.

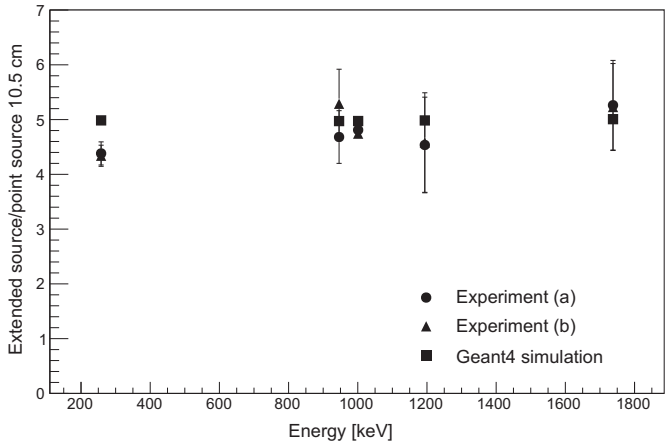

Fig. 6. Extended source/point source efficiency ratio at prominent gamma-ray energies of ^{234}U. The results from two independent experiments (a) and (b) are shown with GEANT4 simulations for the serial dilution measurements described in Sec. 2.3. Results shown are for the 60 mL vial, the second step of the serial dilution process.

were used to correct for extended source efficiency. GEANT4 simulations provide a useful comparison to experimental results, as well as a method to investigate aspects of the detector response which are impossible to observe experimentally.

2.3. Extended source efficiency correction

The efficiency calibration described in Sec. 2.1 was completed using standard point sources, whereas rainwater and seaweed samples were measured in 24 mL, 60 mL, and 120 mL glass vials. Altering the source geometry and composition has a large effect on the efficiency of gamma ray detection; this effect must be quantified for proper data analysis. The corrected efficiency for extended sources can be calculated using Eq. (2), where the correction factor C_s which accounts for the change in detection efficiency is source dependent.

$$\varepsilon_{\text{extended}} = \varepsilon_{\text{point}} \times C_s \tag{2}$$

A sample of purified UO_2Cl_2 crystals, a water soluble uranium salt containing depleted and physically separated ^{238}U obtained

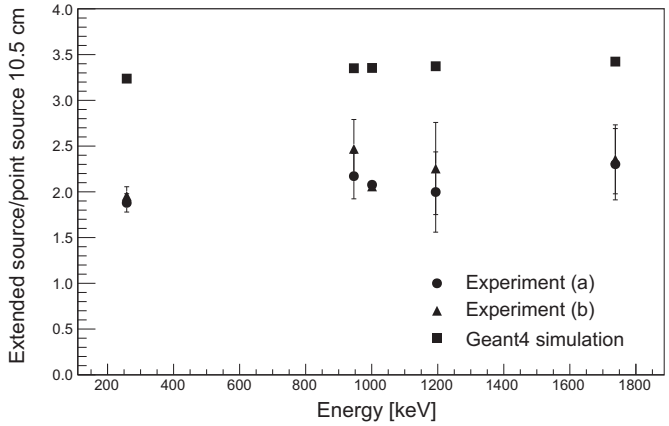

Fig. 7. Extended source/point source efficiency ratio at prominent gamma-ray energies of ^{234}U. The results from two independent experiments (a) and (b) are shown with GEANT4 simulations for the serial dilution measurements described in Sec. 2.3. Results shown are for the 120 mL vial, the final step of the serial dilution process. Experimental results are consistent but show a ~50% discrepancy from GEANT4 simulations attributed to adsorption of UO_2Cl_2 on the walls of the vial.

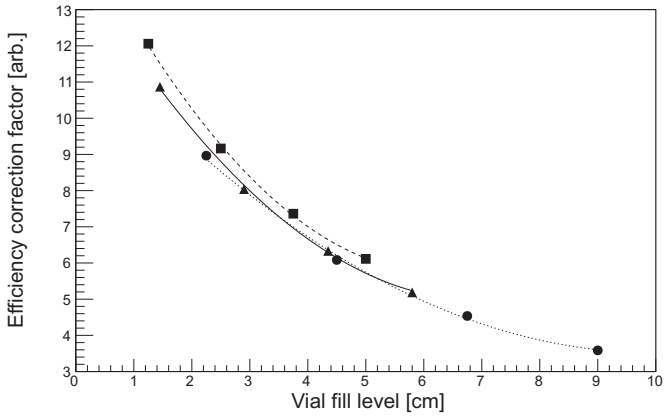

Fig. 8. Extended source efficiency correction curves for the 24 mL [squares, dashed line], 60 mL [triangles, solid line] and 120 mL [circles, dotted line] vials; extended source efficiency is defined in Sec. 2.3 and calculated using Eq. (2). Data points are GEANT4 simulated extended/point source ratios corresponding to the vial being 1/4 full, 1/2 full, 3/4 full and filled to capacity; error bars are smaller than the data points. The curves shown are second order polynomial fits to the ratio of the extended source efficiency to point source efficiency at 10.5 cm with an a vial fill level of x cm.

from the SFU Department of Chemistry was used to construct a point-like source. The point-like source was measured in two positions: 1) placed on the detector can and 2) at 10.5 cm above the detector. Extended sources with identical geometry to those used in the measurements described in Sec. 3.2 and Sec. 3.3 were constructed by dissolving the UO_2Cl_2 point source sample to prepare a series of dilutions which served as standard calibration sources with constant activity distributed in different volumes. The UO_2Cl_2 from the point source was transferred to a 24 mL glass vial, dissolved completely in distilled water, and measured on GEARS. Subsequent serial dilution measurements were performed using 60 mL and 120 mL vials; during each transfer, the smaller vial was thoroughly rinsed into the larger volume with distilled water.

The ^{238}U decay chain up to ^{234}U is in secular equilibrium due to the use of depleted UO_2Cl_2 starting material; thus, the number of excited state ^{234}U atoms populated following the β-decay of ^{234}Pa which decay to the ground state by gamma-ray emission is constant with respect to the measurement duration. To analyze the efficiency of each extended source, the 258.227, 945.94, 1001.03, 1193.73, and 1737.75 keV (National Nuclear Data Center Interactive Chart of Nuclides, 2012) gamma-ray decays of excited states in ^{234}U were measured after each dilution. Following each measurement,

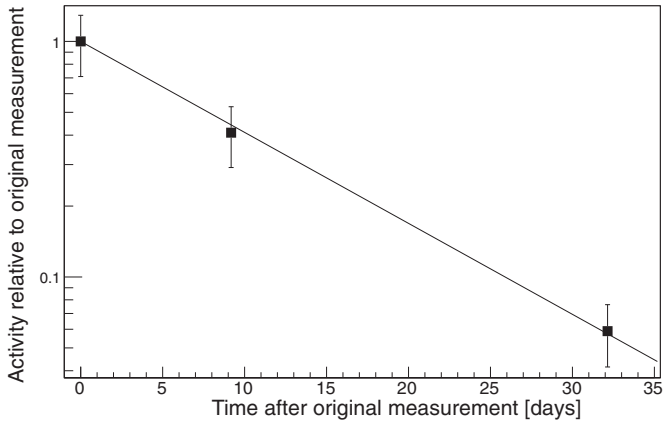

Fig. 9. Activity in North Vancouver seaweed of the 364.489 keV gamma-ray line relative to the original measurement as a function of time. The data were fit using Eq. (3). The best fit lifetime is × days, in agreement with the literature value of 11.5779(7) days (National Nuclear Data Center Interactive Chart of Nuclides, 2012).

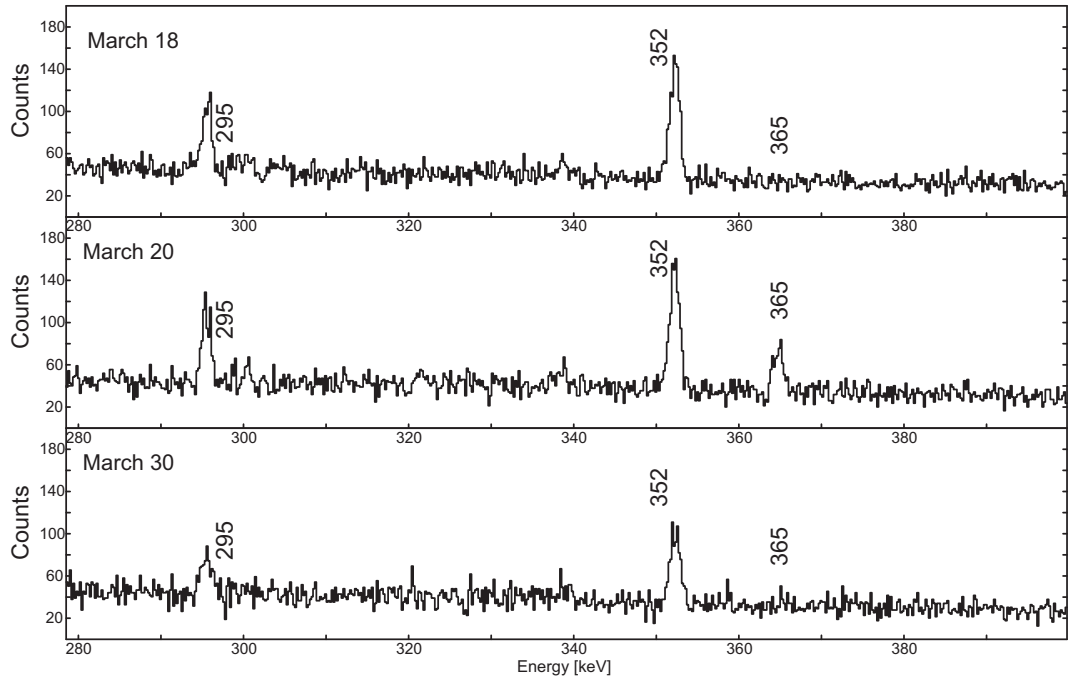

Fig. 10. Three gamma-ray spectra measured by GEARS during the rainwater monitoring campaign. The 364.489 keV peak is characteristic of ^{131}I and indicates its presence in the samples collected at SFU. The 295.224 keV and 351.9 keV peaks are natural background radiation from the ^{238}U decay chain. Damage to the Fukushima Dai-ichi plant occurred on March 11. No ^{131}I was observed in the sample collected on March 18, while the spectrum from the sample collected on March 20 contained the highest measured ^{131}I activity. Rainwater collection was halted shortly after March 30, when ^{131}I content dropped below the detection limit.

the activity ratio with respect to the point source was calculated over this range of energies. Two independent measurements were completed.

The results of the two measurements and the GEANT4 simulations for the 24 mL, 60 mL and 120 mL vials are shown in Figs. 5 and 6, and 7. The two measurements in the 24 mL vial were consistent. GEANT4 simulations of this extended source were completed, and found to be consistent with the experimental values. The measurements in the 120 mL vial were also consistent with one another. However, the experimental results were ~50% below the ratio calculated using GEANT4 simulations. This disagreement could arise from an inhomogeneous distribution of UO_2Cl_2 in the vial due to the formation of so-called radiocolloids or adsorption on the glass walls, phenomena which have been previously observed in dilute solutions of radioactive salts (Tölgyessy et al., 1971). A control experiment to test the adsorption of UO_2Cl_2 on the walls of the glass vials was completed and non-reversible adsorption on glass was observed following the rinsing procedure used to construct the extended sources for calibration.

Every vial used during the rainwater monitoring campaign was filled to capacity and therefore only a single correction factor for each vial size was necessary. However, seaweed samples were measured in all three vials filled to various degrees. GEANT4 simulations were conducted to assess how detection efficiency varied with vial fill level in order to properly correct the seaweed data. Simulations with $E_\gamma = 364.489$ keV were performed with vials 1/4

Table 3
Activity concentration of ^{131}I in rainwater collected at the SFU campus on Burnaby Mountain following the Fukushima accident on March 11, 2011. Errors values at one standard deviation are shown in parentheses, for further details regarding error analysis, see Sec. 2.1. Efficiency correction factors were determined by GEANT4 simulation. The measurement livetime was $\geq$ 99% of the measurement duration. These data are shown in Fig. 11.

Collection date	Measurement livetime [s]	Sample volume [L]	Counts in 364.489 keV ^{131}I photopeak	Efficiency correction factor	Activity concentration [Bq/L]
16 Mar	78020	0.023 (1)	0 (34)	5.89 (2)	0.0 (8)
18 Mar	100945	0.023 (1)	0 (35)	5.89 (2)	0.0 (6)
19 Mar	151045	0.023 (1)	349 (34)	5.89 (2)	4.1 (4)
20 Mar	85465	0.023 (1)	262 (28)	5.89 (2)	5.8 (7)
25 Mar	92145	0.023 (1)	242 (29)	5.89 (2)	4.9 (6)
27 Mar	72109	0.023 (1)	102 (21)	5.89 (2)	2.4 (5)
28 Mar	70045	0.023 (1)	77 (19)	5.89 (2)	2.0 (5)
29 Mar	88231	0.023 (1)	72 (20)	5.89 (2)	1.5 (4)
30 Mar	80068	0.023 (1)	31 (19)	5.89 (2)	0.7 (4)
31 Mar	65534	0.119 (1)	28 (15)	3.242 (12)	0.26 (14)
01 Apr	162184	0.119 (1)	162 (29)	3.242 (12)	0.65 (12)
04 Apr	69455	0.119 (1)	0 (31)	3.242 (12)	0.0 (3)
05 Apr	36567	0.119 (1)	0 (23)	3.242 (12)	0.0 (4)
07 Apr	78797	0.119 (1)	74 (31)	3.242 (12)	0.6 (3)
10 Apr	65568	0.119 (1)	0 (31)	3.242 (12)	0.0 (3)
14 Apr	62703	0.119 (1)	0 (37)	3.242 (12)	0.0 (4)

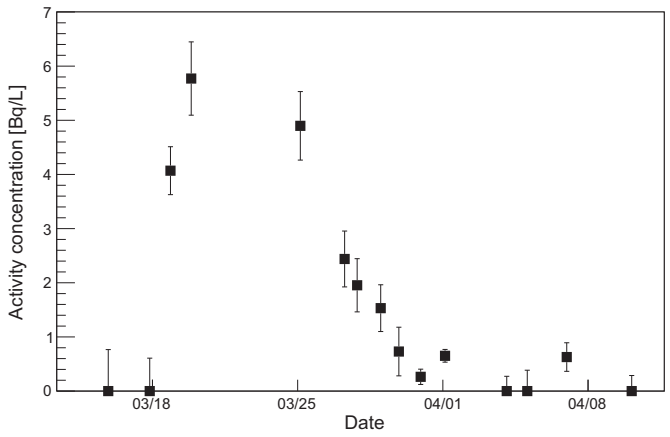

Fig. 11. Time profile of ^{131}I activity concentration in rainwater collected at the SFU campus on Burnaby Mountain following the Fukushima accident. The maximum activity concentration of ^{131}I was observed on March 20, nine days after the tsunami. By April, no more ^{131}I was present in collected rainwater, indicating no continuous releases from the Fukushima reactors. Gaps in the collection correspond to days when there was no rainfall.

full, 1/2 full, 3/4 full and filled to capacity. A least squares fit with a second order polynomial was performed on these data. Efficiency corrections for partially filled vials were made using the correction factor obtained from the fit and Eq. (2). These data and the accompanying fits are shown in Fig. 8.

2.4. Sampling procedure

2.4.1. Rainwater sampling

Rainwater samples were collected at the SFU campus approximately once per day. Following collection, the rainwater was filtered using 110 mm diameter Whatman filter paper to remove particulates and transferred to 24 mL and 120 mL glass vials. The vials were placed on the GEARS detector and measured. The 364.489 keV line indicative of ^{131}I decay was selected for quantitative analysis. Rainwater collection began on March 16, 2011 and continued through April 14, 2011.

2.4.2. Seaweed sampling

Fucus samples were gathered primarily from BMSC on Vancouver Island and from the Burrard Inlet in North Vancouver. The sample collection site from North Vancouver was located near a storm drain, potentially exposing the seaweed to ^{131}I contained in sewage effluent and runoff. Once obtained, samples were rinsed with tap water to remove sand, rocks, aquatic animals and epiphytes from the surface of the seaweed and air dried until most of the rinsing water had evaporated (~4 h). The air-dried seaweed was placed in a commercially available food dehydrator and dried overnight at a temperature of ~70 °C. Samples were ground into a powder using a mortar and pestle and transferred to 24 mL, 60 mL, or 120 mL glass vials and weighed. Seaweed collection began in North Vancouver on March 15, 2011 and at BMSC on March 22.

3. Results

3.1. Monitoring ^{131}I following the Fukushima accident

The presence of ^{131}I was confirmed following the identification of the characteristic 364.489 keV and 284.305 keV gamma rays in environmental samples as well as a lifetime measurement of the 364.489 keV gamma-ray line in a single seaweed sample shown in Fig. 9. To perform the lifetime fit, activity ratios in a single sample were measured as a function of time. The sample used to generate these data was collected on March 28, 2011 in North Vancouver and initially measured on March 31, 2011. The same sample was

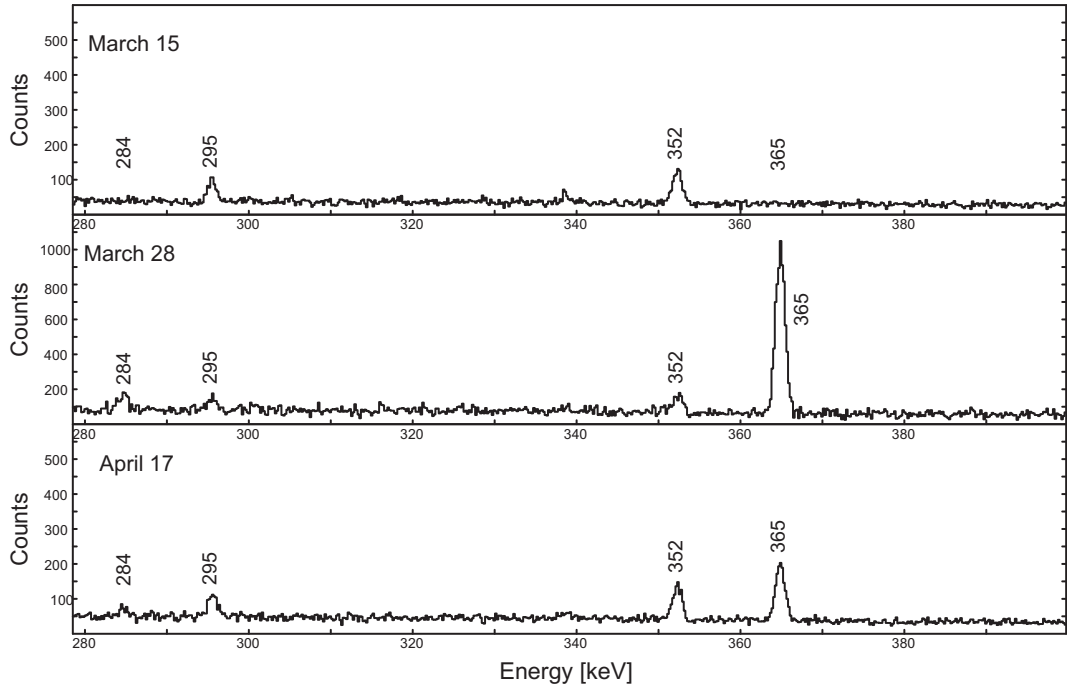

Fig. 12. Three gamma-ray spectra from North Vancouver *Fucus* measured by GEARS during the seaweed monitoring campaign. The 365 keV and 284.305 keV peaks are characteristic of ^{131}I and indicate its presence in the seaweed collected in North Vancouver. The 295.224 keV and 351.9 keV peaks are natural background radiation from the ^{238}U decay chain. No ^{131}I was observed in the sample collected on March 15, while the spectrum from the sample collected on March 28 exhibits two gamma-ray peaks characteristic of ^{131}I loading. There is a marked decrease in ^{131}I activity by mid April, and *Fucus* samples from North Vancouver were not collected past May 10 due to negligible ^{131}I content.

Table 4
Activity concentration of ^{131}I in Bq/kg dry weight from *Fucus* collected in North Vancouver following the Fukushima accident on March 11, 2011, part (a). Errors values at one standard deviation are shown in parentheses, for further details regarding error analysis, see Sec. 2.1. Efficiency correction factors were calculated from the appropriate best fit curves shown in Fig. 8. These data are shown in Fig. 13. The† denotes a single large sample which was divided into three samples measured at different times. The measurement livetime was ≥ 99% of the measurement duration.

Collection date	Collection location	Measurement livetime [s]	Sample mass [g]	Counts in ^{131}I photopeak	Efficiency correction factor	Activity concentration [Bq/kg]
15 Mar	49.3124 N 123.0872 W	83989	3.5693	0 (44)	11.39 (3)	0 (3)
22 Mar	49.3124 N 123.0872 W	66619	3.6629	702 (40)	6.13 (3)	130 (7)
28 Mar	49.3124 N 123.0872 W	9102	29.4580	885 (42)	8.87 (3)	111 (5)
01 Apr	49.3124 N 123.0872 W	5704	13.6534	196 (22)	10.50 (3)	80(9)
05 Apr	49.3124 N 123.0872 W	4757	30.0408	339 (27)	7.41 (2)	94 (8)
10 Apr†	49.3124 N 123.0872 W	8844	7.2440	118 (18)	10.93 (3)	54 (8)
10 Apr†	49.3124 N 123.0872 W	7931	8.8573	142 (19)	9.85 (2)	67 (9)
10 Apr†	49.3124 N 123.0872 W	104618	10.9545	1092 (57)	6.032 (17)	56 (3)

Table 5
Activity concentration of ^{131}I in Bq/kg dry weight from *Fucus* collected in North Vancouver following the Fukushima accident on March 11, 2011, part (b). Errors values at one standard deviation are shown in parentheses, for further details regarding error analysis, see Sec. 2.1. Efficiency correction factors were calculated from the appropriate best fit curves shown in Fig. 8. These data are shown in Fig. 13. The measurement livetime was ≥ 99% of the measurement duration.

Collection date	Collection location	Measurement livetime [s]	Sample mass [g]	Counts in ^{131}I photopeak	Efficiency correction factor	Activity concentration [Bq/kg]
11 Apr	49.3124 N 123.0872 W	20926	45.9654	487 (35)	5.203 (19)	51 (4)
11 Apr	49.3122 N 123.0872 W	20803	71.8451	607 (38)	4.803 (14)	35 (2)
11 Apr	49.3115 N 123.0864 W	69327	31.1776	1238 (57)	8.143 (19)	27.4 (1.1)
11 Apr	49.3111 N 123.0856 W	82553	47.9947	1643 (65)	5.203 (19)	28.6 (1.1)
17 Apr	49.3124 N 123.0872 W	101097	22.7575	1542 (65)	8.97 (2)	26.9 (1.1)
17 Apr	49.3124 N 123.0872 W	102893	22.6537	1170 (59)	9.52 (2)	26.6 (1.3)
25 Apr	49.3124 N 123.0872 W	63226	38.8693	550 (42)	7.167 (17)	9.4 (7)
01 May	49.3124 N 123.0872 W	76177	34.8471	383 (40)	5.16 (2)	9.4 (1.0)
10 May	49.3124 N 123.0872 W	168885	74.2620	652 (50)	8.01 (2)	2.14 (16)

Table 6
Activity concentration of ^{131}I in Bq/kg dry weight from *Fucus* collected at BMSC on Vancouver Island, part (a). Errors values at one standard deviation are shown in parentheses, for further details regarding error analysis, see Sec. 2.1. Efficiency correction factors were calculated from the appropriate best fit curves shown in Fig. 8. The measurement livetime was ≥ 99% of the measurement duration. These data are shown in Fig. 13.

Collection date	Collection location	Measurement livetime [s]	Sample mass [g]	Counts in ^{131}I photopeak	Efficiency correction factor	Activity concentration [Bq/kg]
22 Mar	48.83 N 124.15 W	91250	9.3063	639 (47)	8.90 (2)	29 (2)
25 Mar	48.8370 N 125.1433 W	73278	19.4958	1595 (61)	10.71 (3)	44.9 (1.7)
28 Mar	48.8370 N 125.1433 W	16055	11.2668	354 (30)	9.45 (2)	67 (6)
30 Mar	48.8356 N 125.1366 W	11495	10.1661	115 (19)	9.85 (2)	50 (8)
01 Apr	48.8356 N 125.1366 W	2942	40.2153	96 (15)	6.429 (19)	55 (9)
04 Apr	48.8356 N 125.1364 W	5604	37.6974	160 (20)	6.77 (2)	58 (7)
05 Apr	–	67494	5.6684	218 (33)	11.88 (4)	37 (6)
06 Apr	48.8356 N 125.1366 W	87450	60.3971	1463 (63)	5.203(19)	36.0 (1.5)
08 Apr	48.8356 N 125.1366 W	14942	51.9189	219 (25)	5.203 (19)	36 (4)

Table 7
Activity concentration of ^{131}I in Bq/kg dry weight from *Fucus* collected at BMSC on Vancouver Island, part (b). Errors values at one standard deviation are shown in parentheses, for further details regarding error analysis, see Sec. 2.1. Efficiency correction factors were calculated from the appropriate best fit curves shown in Fig. 8. The measurement livetime was ≥ 99% of the measurement duration. These data are shown in Fig. 13.

Collection date	Collection location	Measurement livetime [s]	Sample mass [g]	Counts in ^{131}I photopeak	Efficiency correction factor	Activity concentration [Bq/kg]
11 Apr	48.8356 N 125.1366 W	73537	48.9233	961 (52)	5.203 (19)	28.7 (1.6)
13 Apr	–	66604	10.9988	326 (37)	9.08 (2)	21 (2)
15 Apr	48.8356 N 125.1366 W	67770	61.9135	891 (51)	5.089 (15)	23.1 (1.3)
17 Apr	48.8356 N 125.1364 W	166602	4.1281	442 (48)	11.16 (3)	23 (3)
19 Apr	–	135982	14.5887	570 (49)	10.81 (4)	16.7 (1.4)
21 Apr	–	100617	10.9104	138 (32)	9.45 (2)	6.4 (1.5)
03 May	48.8356 N 125.1366 W	247374	18.1570	350 (40)	8.87 (3)	3.6 (4)
10 May	48.8356 N 125.1366 W	87681	37.3040	152 (25)	6.651 (19)	2.2 (4)

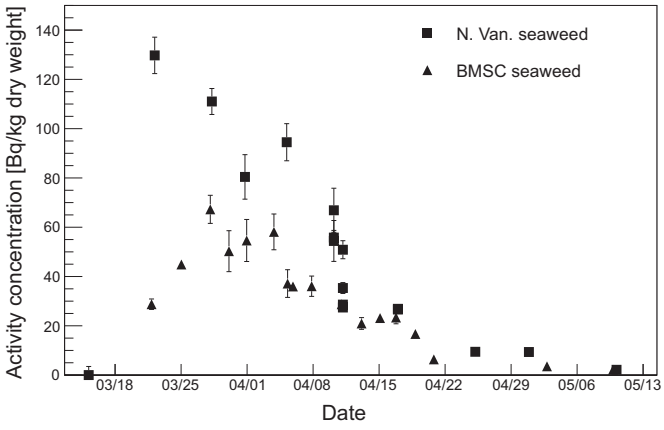

Fig. 13. Time profile of ^{131}I activity concentration in *Fucus* collected in North Vancouver [squares] and *Fucus* collected at BMSC [triangles]. Maximum measured activity was observed on March 22 for seaweed collected in North Vancouver and March 28 for seaweed collected at BMSC, 11 and 17 days after the tsunami, respectively. By mid-May, there was very little observed ^{131}I activity in seaweed, and the monitoring campaign was halted.

re-measured on April 9, 2011 and May 4, 2011. The data was fit with the exponential function given in Eq. (3).

$$\frac{A(t)}{A(t_0)} = e^{-(t-t_0)/\tau} \tag{3}$$

where $A(t)$ is the activity at time t, $A(t_0)$ is the activity measured on t_0 = March 31, 2011, t is the time since t_0 in days, and τ is the best fit lifetime in days. A re-measurement of the sample was performed on November 9, 2012 and no ^{131}I was observed. The decrease to zero ^{131}I activity justifies the exclusion of a constant in the exponential fit. The best fit lifetime was $\tau = 11.2(1.1)$ days, in agreement with the literature value of 11.5779(7) days (National Nuclear Data Center Interactive Chart of Nuclides, 2012).

Activity concentrations of ^{131}I were obtained from integration of the 364.489 keV gamma-ray line. The activity concentration in rainwater and seaweed samples at the collection time was corrected for measurement delay, ^{131}I half-life, the efficiency of the detector, and the known branching ratio (0.815) of the 364.489 keV gamma ray (Khazov et al., 2006).

3.2. Rainwater

Iodine-131 was first observed in rainwater on March 19, 2011, eight days after the tsunami damaged the reactors at the Fukushima Dai-ichi plant on March 11. Maximum activity was observed on March 20, nine days after the tsunami. The activity of ^{131}I in rainwater was below the detection limit of GEARS by early April, 2011 and was no longer monitored once the 364.489 keV gamma ray was consistently not observed. Several gamma-ray spectra illustrating the change in activity measured during the rainwater monitoring campaign are shown in Fig. 10, the extended source efficiency corrected data collected during the rainwater monitoring campaign are contained in Table 3, and a time profile of ^{131}I concentration in Burnaby Mountain rainwater is shown in Fig. 11.

Table 9
Maximum measured ^{131}I activity concentration in Bq/kg dry weigh for *Fucus* collected following the Chernobyl accident (Druehl et al., 1988) compared to the current work following the Fukushima accident. Errors values at one standard deviation are shown in parentheses.

Sample location	Chernobyl [Bq/kg]	Current work [Bq/kg]
Vancouver area	4750 (380)	130 (7)
BMSC	4930 (680)	67 (6)

3.3. Seaweed

The maximum measured ^{131}I activity concentration occurred on March 22 for local seaweed and on March 28 for seaweed from BMSC, 11 and 17 days after the earthquake, respectively. Iodine-131 concentration in seaweed demonstrates a significant positive correlation with precipitation, and ^{131}I levels in *Fucus* have been shown to reflect observed levels in rain (Druehl et al., 1988). Seawater samples in Korea collected at the surface and at depths up to 2000 m did not contain measurable amounts of ^{131}I (Kim et al., 2012), which indicates that rainwater is the primary source of ^{131}I uptake in *Fucus*. By mid-May, one month after ^{131}I was last observed in rainwater, the ^{131}I content in the seaweed samples had decreased to below 5 Bq/kg dry weight, therefore the seaweed monitoring campaign was halted. Gamma-ray spectra showing the change in ^{131}I content measured in North Vancouver seaweed are shown in Fig. 12. The extended source efficiency corrected data collected from North Vancouver seaweed over the course of the monitoring campaign are shown in Tables 4 and 5; the corresponding data from the BMSC are shown in Tables 6 and 7. All activity concentrations and mass measurements for seaweed samples are reported for dry weight. Time profiles of ^{131}I activity concentration in North Vancouver and BMSC seaweed samples are shown in Fig. 13

Two samples of *Macrocystis pyrifera* (giant kelp), two samples of *Fucus*, and one sample of *Pyropia fallax*, formerly known as *Porphyra fallax* (Sutherland et al., 2011) collected in Bella Bella, BC were received and processed following the procedure outlined above, the data are shown in Table 8.

4. Discussion

The discrepancy between GEANT4 simulations and the extended source calibration was accounted for when constructing the time profiles shown in Figs. 11 and 13 and Tables 3–7 For the rainwater

Table 8
Activity concentration in Bq/kg dry weight of a variety of seaweed species collected from Bella Bella, BC on 1 April 2011 following the Fukushima accident. Errors values at one standard deviation are shown in parentheses, for further details regarding error analysis, see Sec. 2.1. Efficiency correction factors were calculated from the appropriate best fit curves shown in Fig. 8. The measurement livetime was $\geq$ 99% of the measurement duration. The variation between collected samples suggest different accumulation rates of ^{131}I as a function of seaweed size, age, or habitat.

Species	Measurement livetime [s]	Sample mass [g]	Counts in ^{131}I photopeak	Efficiency correction factor	Activity concentration [Bq/kg]
Macrocystis pyrifera (a)	25422	3.5065	145 (22)	9.26 (2)	59 (9)
Macrocystis pyrifera (b)	48048	2.9702	340 (34)	9.85 (2)	90 (9)
Fucus (a)	14564	9.8619	223 (25)	8.90 (2)	63 (7)
Fucus (b)	71949	7.0597	564 (44)	10.70 (3)	40 (3)
Pyropia fallax	21025	2.4901	26 (13)	8.07 (2)	15 (8)

samples, only the 24 mL and 120 mL vials were used during the monitoring campaign. The GEANT4 simulations and extended source measurement using the 24 mL vial were consistent, therefore GEANT4 simulations were accepted as accurate for the 24 mL vial efficiency corrections. The 120 mL vials were only used for rainwater measurements following March 31, 2011 when the ^{131}I content was approaching negligible levels. Seven measurements were taken using the 120 mL vials; four of these were below the detection limit of GEARS and the other three were corrected to below 1 Bq/L using the GEANT4 simulations. Because the activity concentration measured in these cases was very low, a large uncertainty in the extended source correction due to adsorption on the glass does not significantly impact the interpretation of the results. For the *Fucus* samples which were not in solution, adsorption effects on the glass walls of the vials was not considered.

Iodine-131 was first observed in rainwater at SFU on March 19 and maximum activity concentration was measured on March 20. This result is consistent with results reported from Washington state where airborne ^{131}I activity concentration was first observed on March 18, with a maximum occurring on March 20 (Diaz Leon et al., 2011). Airborne ^{131}I activity concentration in Washington state was higher than what was observed in Europe, the Canary Islands, and South Korea. Concurrent rainwater measurements at SFU demonstrate larger ^{131}I activity concentration compared to values reported in Europe and South Korea (Ioannidou et al., 2012; Kim et al., 2012; Perrot et al., 2012).

The results of the current work were also compared to measurements performed following the Chernobyl nuclear disaster (Druehl et al., 1988). Similar experimental conditions (using a shielded HPGe detector, measuring *Fucus*) allow for a direct comparison of ^{131}I loading in *Fucus* samples collected from the Vancouver area and BMSC; the results are shown in Table 9. The ^{131}I activity concentration observed in seaweed was an order of magnitude less than what was observed following Chernobyl. Dose estimates for Canadian residents following Chernobyl were estimated to be $\sim$1 μSv (Snell and Howieson, 1991). The observed ^{131}I activity in the current study implies an upper limit for the radiation dose attributable to releases from Fukushima of $\sim$0.1 μSv, an order of magnitude less than what was reported following Chernobyl. For comparison, the annual effective dose from naturally occurring radiation in Vancouver is 1.3 mSv (Canadian Nuclear Safety Commission Radiation Doses, 2013).

5. Conclusions

The measured ^{131}I activity in seaweed in the current work is an order of magnitude less than what was observed in BC following Chernobyl. The maximum observed ^{131}I concentration in rainwater of 5.8(7) Bq/L is a factor of 16 lower than the government action levels set on drinking water by Health Canada following a nuclear emergency (Health Canada, 2000). The estimated dose in Vancouver attributed to Fukushima is four orders of magnitude less than the annual dose from background radiation. Therefore, the short- and long-term impact of Fukushima on human health and the environment in Canada is expected to be insignificant.

^{131}I was observed in rainwater samples for $\sim$1 month following the Fukushima accident, while ^{131}I activity in *Fucus* samples collected in southwest B.C. was observed for $\sim$2 months. The observations made in the current work confirm that *Fucus* can be used as an efficient system to measure the distribution of small amounts of ^{131}I in the environment, as previously proposed (Druehl et al., 1988). This result is particularly relevant when governments and coastal communities need to choose an indicator source and monitoring timeframe when ^{131}I contamination in the environment is a concern.

Additionally, the current work establishes GEARS as a high-precision tool for radiochemical analysis. A well shielded, absolutely calibrated HPGe detector is a powerful instrument for detecting small amounts of radiation as demonstrated by the low levels of activity measured with high precision in rainwater and seaweed. There is significant interest in monitoring and quantifying radioisotopes present in the environment, and the Nuclear Science group at SFU is actively pursuing this research opportunity.

Acknowledgments

The authors would like to thank NSERC for funding the work presented (SAPIN/371656-2010), the B.C. Centre for Disease control for providing the low-activity lead shield, and Dr. D. Leznoff for providing the uranium salts. This project was completed with the cooperation and support of Dr. M. Pinto, VP Research, Simon Fraser University.

References

Agostinelli, S., et al., 2003. Geant4-a simulation toolkit. Nuc. Inst. Meth. A. 6 (3), 250–303.
Allison, J., et al., 2006. Geant4 developments and applications. IEEE Trans. Nucl. Sci. 53 (1), 270–278.
Canadian Nuclear Safety Commission Radiation Doses. http://www.cnsc-ccsn.gc.ca/eng/readingroom/radiation/radiation_doses.cfm.
Diaz Leon, J., et al., 2011. Arrival time and magnitude of airborne fission products from the Fukushima, Japan, reactor incident as measured in Seattle, WA, USA. J. Env. Rad. 102, 1032–1038.
Druehl, L.D., Cackette, M., D'Auria, J.M., 1988. Geographical and temporal distribution of iodine-131 in the brown seaweed fucus subsequent to the Chernobyl incident. Mar. Biol. 98, 125–129.
England, T.R., Rider, B.F., 1994. Evaluation and Compilation of Fission Product Yields 1993. ENDF-349 LA-UR-94-3106.
Health Canada, 2000. Canadian Guidelines for the Restriction of Radioactively Contaminated Food and Water Following a Nuclear Emergency.
Ioannidou, A., et al., 2012. Fukushima fallout at Milano, Italy. J. Env. Rad. 114, 119–125.
Khazov, Yu., et al., 2006. Nucl. Data Sheets 107, 2715.
Kim, C.-K., et al., 2012. Radiological impact in Korea following the Fukushima nuclear accident. J. Env. Rad. 111, 70–82.
Kim, I.J., Park, C.S., Choi, H.D., 2003. Absolute calibration of ^{60}Co by using sum peak method and an HPGe detector. Appl. Radiat. Isot. 58, 227–233.
Knoll, G.F., 2000. Radiation Detection and Measurement, third ed. John Wiley and Sons, US.
López-Pérez, M., et al., 2013. Arrival of radionuclides released by the Fukushima accident to Tenerife (Canary Islands). J. Env. Rad. 116, 180–186.
Malain, D., et al., 2012. An evaluation of the natural radioactivity in Andaman beach sand samples of Thailand after the 2004 tsunami. Appl. Radiat. Isot. 70, 1467–1474.
Manolopoulou, M., et al., 2011. Radioiodine and radiocesium in Thessaloniki, Northern Greece due to the Fukushima nuclear accident. J. Env. Rad. 102, 796–797.
National Nuclear Data Center Interactive Chart of Nuclides. http://www.nndc.bnl.gov/chart/.
Perrot, F., et al., 2012. Evidence of ^{131}I and ^{134,137}Cs activities in Bordeaux, France due to the Fukushima nuclear accident. J. Env. Rad. 114, 61–65.
Pham, M.K., et al., 2012. Detection of Fukushima Diichi nuclear power plant accident radioactive traces in Monaco. J. Env. Rad. 114, 131–137.
Snell, V.G., Howieson, J.Q., 1991. Chernobyl-a Canadian Perspective. Atomic Energy of Canada Limited, CANDU Operations.
Sutherland, J., et al., 2011. A new look at an ancient order: generic revision of the Bangiales (Rhodophyta). J. Phycol. 47, 1131–1151.
Tölgyessy, J., Varga, S., Krivan, V., 1971. Nuclear Analytical Chemistry I: Introduction to Nuclear Analytical Chemistry. Publishing House of the Slovak Academy of Sciences, Bratislava, Slovakia.